

Spontaneous generation and impact of inertia-gravity waves in a stratified, two-layer shear flow

P. D. Williams and P. L. Read

Atmospheric, Oceanic and Planetary Physics, Clarendon Laboratory, University of Oxford, UK

T. W. N. Haine

Department of Earth and Planetary Sciences, Johns Hopkins University, Baltimore, USA

Received 26 August 2003; revised 12 November 2003; accepted 17 November 2003; published 19 December 2003.

[1] Inertia-gravity waves exist ubiquitously throughout the stratified parts of the atmosphere and ocean. They are generated by local velocity shears, interactions with topography, and as geostrophic (or spontaneous) adjustment radiation. Relatively little is known about the details of their interaction with the large-scale flow, however. We report on a joint model/laboratory study of a flow in which inertia-gravity waves are generated as spontaneous adjustment radiation by an evolving large-scale mode. We show that their subsequent impact upon the large-scale dynamics is generally small. However, near a potential transition from one large-scale mode to another, in a flow which is simultaneously baroclinically-unstable to more than one mode, the inertia-gravity waves may strongly influence the selection of the mode which actually occurs. **INDEX TERMS:** 3210 Mathematical Geophysics: Modeling; 3220 Mathematical Geophysics: Nonlinear dynamics; 3346 Meteorology and Atmospheric Dynamics: Planetary meteorology (5445, 5739). **Citation:** Williams, P. D., P. L. Read, and T. W. N. Haine, Spontaneous generation and impact of inertia-gravity waves in a stratified, two-layer shear flow, *Geophys. Res. Lett.*, 30(24), 2255, doi:10.1029/2003GL018498, 2003.

1. Introduction

[2] Like many physical systems, fluids often exhibit the coexistence of motions on a wide range of space and time scales. Correspondingly, the linear normal modes of the governing Navier-Stokes equations generally have spatio-temporal structures which fall naturally into distinct classes, when categorized according to the fundamental dynamical mechanisms which permit their existence. This property of the fluid equations was first identified by *Margules* [1893], who derived two species of solutions to Laplace's tidal equations. He named his solutions "Wellen erster Art" (waves of the first type) and "Wellen zweiter Art" (waves of the second type), which we now know more familiarly as inertia-gravity and Rossby waves.

[3] Characteristic wavelengths, intrinsic frequencies and propagation speeds of inertia-gravity and Rossby waves differ by at least an order of magnitude, in both the atmosphere and ocean. A convenient, often tacit, assumption is that mutual nonlinear interactions between the scale-separated modes are negligible. This justifies the use of a

reduced-dimensional description of the fluid system based upon a projection onto its *slow manifold* [Leith, 1980], a sub-surface of the full phase space upon which inertia-gravity mode amplitudes are identically zero. *Benney* [1977] has shown that a resonant triad interaction between two short waves and one long wave is possible if the phase speed of the long wave is equal to the group speed of the short waves, however. The physical interpretation is that the energy of the short modes, which travels at their group speed, does not drift relative to the phase of the long mode, a requirement which evidently allows a resonant reinforcement of the energy transfer. The typical dispersion curves plotted in Figure 1 show that—in principle, at least—the phase speed of a Rossby wave can match the group speed of a gravity wave. This challenges the assumption that the wave-wave interaction is always negligible.

[4] Laboratory observations of systematic inertia-gravity wave generation by evolving quasi-geostrophic modes were reported by *Lovegrove et al.* [2000]. This finding meant that the interaction could be investigated in a real fluid, without recourse to the ad hoc theoretical idealizations typically made in studies of highly truncated models [e.g., *Lorenz*, 1986]. The present study is an extension of the work of *Lovegrove et al.* [2000] (Section 2). We employ a high-resolution numerical model to investigate the mechanism by which the inertia-gravity waves are generated in the laboratory experiment (Section 3), and then we incorporate a stochastic parameterization of the inertia-gravity waves into the model in order to assess their impacts upon the large-scale flow (Section 4). We end with a statement of our conclusions and a brief discussion in Section 5.

2. The Rotating, Two-Layer Annulus Experiment

[5] In the present laboratory experiments, the fluid occupies the annular domain defined in cylindrical coordinates (r, θ, z) by $0 < z < 25.00$ cm, 6.25 cm $< r < 12.50$ cm and $0 < \theta \leq 2\pi$. The domain is filled with equal volumes of two immiscible liquids (water, and a mixture of d-limonene and CFC-113) whose densities differ by around 0.5%, to give a well-defined equilibrium interface at $z = 12.50$ cm. The base at $z = 0$ and sidewalls at $r = 6.25$ cm, 12.50 cm are made to rotate about the axis of symmetry under computer control, and the lid at $z = 25.00$ cm is made to rotate *relative to the base*. This differential lid rotation provides the velocity shear across the interface required for the generation of a large-scale mode due to baroclinic instability, if the background rotation is large enough. For the experiments

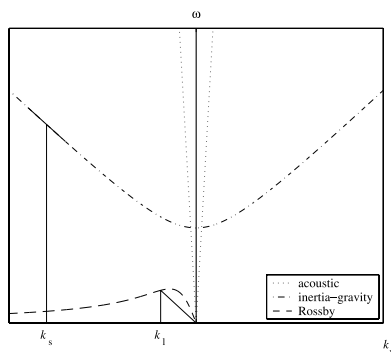


Figure 1. Schematic dispersion curves for three different zonally-propagating shallow-water wave modes, showing intrinsic angular frequency ω as a function of zonal (East-West) wavevector k_x . The Rossby wave chord slope at the long wavevector k_1 is equal to the inertia-gravity wave tangent slope at the short wavevector k_s , leading to the possibility of a resonant triad interaction (see text). Acoustic modes are too fast to take part in such an interaction, which justifies filtering acoustic modes from general circulation models.

described herein, the typical Froude number, Rossby number, Reynolds number, Ekman number and interfacial tension number are $F \sim 10$, $Ro \sim 0.1$, $Re \sim 10^3$, $Ek \sim 10^{-6}$ and $I \sim 0.1$, respectively [Williams, 2003].

[6] The apparatus is viewed from above by a colour video camera on the axis of symmetry around 2 m above the annulus, and is illuminated from below by a bright white lamp. The base, lid and fluids are transparent and colourless, allowing the passage of light through the apparatus. The system is viewed through crossed polaroids, and the lower-layer liquid is optically active, giving a direct relationship between colour observed by the camera and lower layer depth (see Hart and Kittleman [1986] for more details).

[7] A typical still from the video footage is shown in Figure 2. The large-scale wave, of azimuthal wavenumber 2, has arisen from a baroclinic instability and drifts slowly around the annulus. Two trains of deep-water inertia-gravity waves (IGWs) have developed and are superimposed in the troughs of the shallow-water large-scale mode. Their wavelengths, intrinsic periods and amplitudes are each a factor of around 10 smaller than those of the large-scale mode. The structure of the IGW trains bears a striking resemblance to those generated during the spontaneous adjustment process in the high-resolution atmospheric simulations of O’Sullivan and Dunkerton [1995], despite the differences in length and time scales between the atmosphere and laboratory.

3. Numerical Annulus Model

[8] There are two candidate generation mechanisms for the IGWs observed in the laboratory, as in the free atmosphere. The first is the spontaneous emission radiation mechanism [Ford et al., 2000], and the second is a Kelvin-Helmholtz shear instability. In order to examine which of the two mechanisms may be responsible in the laboratory, the horizontal velocity fields are needed, which

are unavailable from the experiment. To this end, we simulate the large-scale laboratory flow using a two-layer quasi-geostrophic annulus model known as *QUAGMIRE* [Williams, 2003]. The model integrates the quasi-geostrophic potential vorticity equations in both layers, with parameterized Ekman pumping and suction velocities at the lid, base and interface. Cylindrical geometry is used, and the effects of interfacial tension are included. We use a grid of 96 points in azimuth and 16 in radius. We perform the timestepping using the potential vorticity tendency equations in physical space, but transform to normal mode space once per timestep to obtain the streamfunction by inverting the potential vorticity. At the sidewall boundaries, we impose impermeability on the eddy flow components, and no-slip boundary conditions on the mean-flow correction component.

[9] Ageostrophic IGWs are filtered out of the model by construction, and so the model velocity fields allow us to assess the incipient generation of IGWs by a pure quasi-geostrophic mode. A typical model lower layer depth field is shown in Figure 3a, for comparison with the laboratory image in Figure 2 which was obtained with similar background and differential rotation rates. The model wave amplitudes, phase speeds, and zonal wavenumbers agree reasonably well with those observed in the laboratory [Williams, 2003].

[10] Ford [1994] derived an equation which indicates the local strength of spontaneous emission radiation in barotropic shallow water:

$$\left(\frac{\partial^2}{\partial t^2} + f^2 - gH\nabla^2 \right) \frac{\partial h}{\partial t} = \frac{\partial}{\partial t} \nabla \cdot \mathbf{F} + f \mathbf{k} \cdot \nabla \times \mathbf{F} + \frac{g}{2} \frac{\partial}{\partial t} \nabla^2 h^2, \quad (1)$$

where

$$\mathbf{F} = \mathbf{u} \nabla \cdot (h\mathbf{u}) + (h\mathbf{u} \cdot \nabla) \mathbf{u}. \quad (2)$$

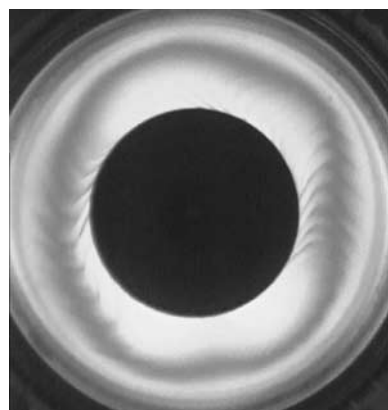


Figure 2. Typical image captured by a video camera viewing the laboratory annulus from above. In the original colour image, the high intensity region near the inner sidewall appears blue and corresponds to an elevated lower layer depth of around $z = 13$ cm, and the high intensity region near the outer sidewall appears yellow and corresponds to a reduced depth of around $z = 11$ cm. The relatively dim region in between appears red and corresponds to lower layer depths close to the undisturbed value of $z = 12.5$ cm.

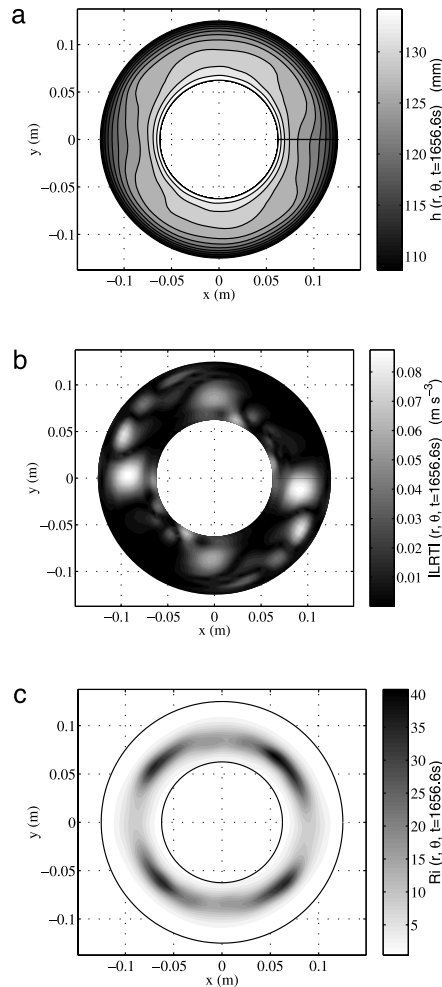


Figure 3. (a) Lower layer depth, (b) Lighthill Radiation Term magnitude, and (c) Richardson number, from a simulation of an azimuthal wavenumber 2 flow corresponding to the laboratory image of Figure 2. The quasi-geostrophic annulus model described in Section 3 was used to produce these diagrams.

Here, $f = 2\Omega$ is the Coriolis parameter, g is the acceleration due to gravity, h is the instantaneous layer depth, with a mean value of H , \mathbf{u} is the horizontal velocity field, and \mathbf{k} is the unit vertical vector. The left side of equation (1) is the linear IGW operator acting on $\partial h / \partial t$. The right side contains all of the nonlinear terms, which we refer to collectively as the Lighthill Radiation Term (LRT), as Ford’s analysis was an extension of the work of *Lighthill* [1952] on the generation of acoustic modes. Though derived using a shallow water assumption, we assert that the same LRT formula applies to the deep water limit, which is more appropriate for the short waves in the laboratory. This is reasonable, since whether or not an evolving, large-scale mode will generate IGWs is not expected to depend upon whether they would propagate in deep or shallow water, if emitted.

[11] Figure 3b shows a plot of LRT for the lower annulus layer, derived from the model velocity fields and lower layer depth at the time of the flow in Figure 3a (g is replaced with the reduced gravity g' in (1) to account for the stratification). Ford argued that regions where LRT is large

in magnitude should also be regions of significant IGW production by the spontaneous emission mechanism. By comparing Figures 2 and 3b we see that the magnitude of LRT has maxima at just those regions where we observe laboratory IGWs. There are smaller, subsidiary maxima in LRT at other locations, but presumably LRT has to be large enough to overcome dissipative effects—which are not included in Ford’s theory—before generation actually occurs. The correlation between regions of laboratory IGW production and regions of subcritical model Richardson number is poor, as shown in Figure 3c. The Richardson number drops below unity only near the outer sidewall, which is not an observed generation region. We conclude, therefore, that spontaneous emission, rather than a Kelvin-Helmholtz shear instability, is responsible for the production of the observed laboratory IGWs. This conclusion has been verified at a range of Froude numbers (from 5 to 20), corresponding to a spectrum of different dominant azimuthal wavenumbers (1, 2 and 3).

[12] In the classic Rossby geostrophic adjustment problem, two IGW trains are emitted in opposite directions so that the total ageostrophic component is zero at the source region. In our experiment, however, all waves are superimposed on a strong zonal flow. Any IGWs which are emitted in the retrograde direction (i.e., against the background flow) can therefore appear to propagate in the prograde direction when viewed by our camera in the frame of the annulus base. This is consistent with our observations, which show a single train of unidirectional IGWs (e.g., Figure 2). The Rossby-Kelvin instability identified by *Sakai* [1989] can be discounted as the cause of the IGW emission we observe, since this resonant instability occurs only for Froude numbers $F \approx 0.7$, which is much smaller than the Froude numbers achieved in the current study.

4. Stochastic Resonance

[13] To explore the impact of the IGWs on the large-scale flow we perform a second model calculation, this time with a random small-amplitude anomaly added to the right side of the model quasi-geostrophic potential vorticity equations for both layers. These new terms are intended to mimic the potential vorticity anomalies induced by the IGWs in the laboratory, which occur almost at the scale of the model gridspacing. Unlike in the laboratory, the stochastically-parameterized IGWs are global, i.e., they are included everywhere, not just in those places at which LRT is large. This may strengthen the correspondence between the model, and the atmosphere and ocean, in which IGWs are perhaps more ubiquitous than in the laboratory. At each gridpoint and timestep, a random number is drawn from a uniform distribution, with a width chosen such that the resulting small-scale interface perturbations have a root-mean-square amplitude similar to those in the laboratory (i.e., around one millimetre). The effects of the parameterized IGWs on the evolution of the large-scale mode are generally small: wave speeds and wavenumbers are unaltered, and there is little change in amplitude.

[14] In some cases, however, the IGWs were found to exert a strong influence on the balanced flow. To illustrate this, a model run was performed with the amplitude of the noise terms slowly increasing with time, after allowing an

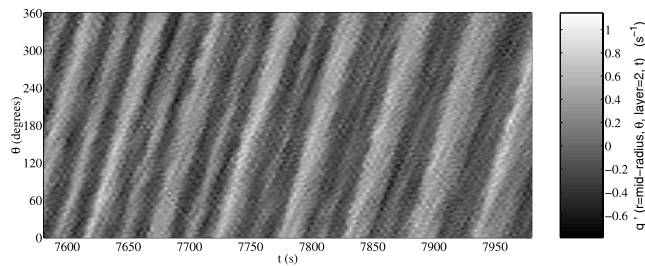


Figure 4. Hovmüller diagram, showing a mid-radius azimuth-time contour plot of perturbation potential vorticity in the lower layer, at the time of a spontaneous transition from azimuthal wavenumber 2 to 1.

azimuthal wavenumber 2 mode to equilibrate in the absence of noise. When a critical noise amplitude was reached—which was still small compared with the amplitude of the background large-scale mode—a spontaneous transition occurred to a large-scale mode with azimuthal wavenumber 1. Potential vorticity as a function of time and azimuthal angle, at the time of the transition, is shown in Figure 4. Such transitions were never observed in the absence of the stochastic forcing, and were not reversed if the noise was gradually decreased back to zero.

[15] These spontaneous transitions occurred when the linear growth rates of the two large-scale modes involved in the transition were similar, i.e., the system was close to a parameter space wavenumber transition curve in a region of intransitive multistability. The phenomenon which allows a small (stochastic) forcing to produce a large (resonant) response is known as *stochastic resonance*, and has been observed before in numerical models of rapidly-rotating barotropic fluid systems [e.g., *De Swart and Grasman, 1987*].

[16] Further evidence to support these model findings comes from the present laboratory experiments. By varying the interfacial tension between the two layers, using a surfactant, we have been able to run experiments in which the large-scale baroclinic mode is not significantly altered, but the small-scale IGWs are greatly suppressed. This is possible because the effects of interfacial tension are scale-selective, affecting the dynamics of short scales much more than long scales. In such laboratory experiments, the large-scale flow was found to exhibit a reluctance to undergo wavenumber transitions when the flow was devoid of IGWs, but more readily underwent such transitions when IGWs were present.

5. Conclusions

[17] We have observed the spontaneous generation of inertia-gravity waves by an evolving large-scale flow in the laboratory. The times and spatial locations at which inertia-gravity waves were observed appear to be well-predicted by the formula due to Lighthill and Ford, and very poorly predicted by analyses based on a critical Richardson number. Shear instability therefore seems unlikely as the source, and we conclude that the observed short-scale waves are most likely generated as spontaneous emission radiation by the large-scale mode.

[18] We have investigated the impact of the short waves on the long waves by using a numerical model of the large-

scale flow with a stochastic inertia-gravity wave parameterization. In general, the impact is small, but we have identified circumstances in which stochastic resonance allows small-amplitude inertia-gravity waves to interact nonlinearly with the balanced flow in a profound way, by forcing spontaneous transitions between balanced modes and influencing long-term mode selection.

[19] The large-scale waves in the laboratory are prototypes of synoptic tropospheric and mesoscale oceanic disturbances. It is therefore likely that small-amplitude, small-scale inertia-gravity waves in the atmosphere and ocean might resonate stochastically to force significant changes to the large-scale balanced flow. This finding adds to the evidence [e.g., *Palmer, 2001*] that deterministic parameterizations of inertia-gravity waves in weather and climate models may be unable to capture the full details of the nonlinear interactions. The present results suggest that certain aspects of the interaction can only be captured by a stochastic parameterization or, presumably, by an explicit representation of the inertia-gravity waves. There is, therefore, a strong case for carrying out further research regarding stochastic representations of sub-grid scale processes in general circulation models.

[20] **Acknowledgments.** PDW acknowledges support under a research studentship from the UK Natural Environment Research Council, held at the University of Oxford, with award reference number GT04/1999/AS/0203.

References

- Benney, D. J., A general theory for interactions between short and long waves, *Stud. Appl. Math.*, 56, 81–94, 1977.
- De Swart, H. E., and J. Grasman, Effect of stochastic perturbations on a low-order spectral model of the atmospheric circulation, *Tellus*, 39(A), 10–24, 1987.
- Ford, R., Gravity wave radiation from vortex trains in rotating shallow water, *J. Fluid Mech.*, 281, 81–118, 1994.
- Ford, R., M. E. McIntyre, and W. A. Norton, Balance and the slow quasi-manifold: Some explicit results, *J. Atmos. Sci.*, 57, 1236–1254, 2000.
- Hart, J. E., and S. Kittelman, A method for measuring interfacial wave fields in the laboratory, *Geophys. Astrophys. Fluid Dyn.*, 36, 179–185, 1986.
- Leith, C. E., Nonlinear normal mode initialization and quasi-geostrophic theory, *J. Atmos. Sci.*, 37, 958–968, 1980.
- Lighthill, M. J., On sound generated aerodynamically. I: General theory, *Proc. R. Soc. Lond.*, 211, 564–587, 1952.
- Lorenz, E. N., On the existence of a slow manifold, *J. Atmos. Sci.*, 43(15), 1547–1557, 1986.
- Lovegrove, A. F., P. L. Read, and C. J. Richards, Generation of inertia-gravity waves in a baroclinically unstable fluid, *Q. J. R. Meteorol. Soc.*, 126, 3233–3254, 2000.
- Margules, M., Luftbewegungen in einer rotierenden Sphäroidschale, *Sitzungsberichte der Kaiserliche Akad. Wiss. Wien*, 102, 11–56, 1893.
- O’Sullivan, D., and T. J. Dunkerton, Generation of inertia-gravity waves in a simulated life cycle of baroclinic instability, *J. Atmos. Sci.*, 52(21), 3695–3716, 1995.
- Palmer, T. N., A nonlinear dynamical perspective on model error: A proposal for non-local stochastic-dynamic parameterization in weather and climate prediction models, *Q. J. R. Meteorol. Soc.*, 127, 279–304, 2001.
- Sakai, S., Rossby-Kelvin instability: A new type of ageostrophic instability caused by a resonance between Rossby waves and gravity waves, *J. Fluid Mech.*, 202, 149–176, 1989.
- Williams, P. D., Nonlinear interactions of fast and slow modes in rotating, stratified fluid flows, D. Phil. thesis, University of Oxford, 2003.

P. D. Williams and P. L. Read, Atmospheric, Oceanic and Planetary Physics, Clarendon Laboratory, Parks Road, Oxford, OX1 3PU, UK. (williams@atm.ox.ac.uk)

T. W. N. Haine, Department of Earth and Planetary Sciences, Johns Hopkins University, Baltimore, USA.